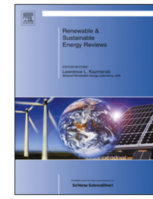
Renewable and Sustainable Energy Reviews 36 (2014) 247–255

Contents lists available at ScienceDirect

Renewable and Sustainable Energy Reviews

journal homepage: www.elsevier.com/locate/rser



Key technologies of VSC-HVDC and its application on offshore wind farm in China

Jie Wu [a,*], Zhi-Xin Wang [a], Lie Xu [b], Guo-Qiang Wang [a]

[a] *Department of Electrical Engineering, Shanghai Jiao Tong University, 200240 Shanghai, China*
[b] *School of Electronics, Electrical Engineering and Computer Science, Queen's University of Belfast, UK*

ARTICLE INFO

Article history:
Received 10 September 2012
Received in revised form
13 April 2014
Accepted 27 April 2014
Available online 20 May 2014

Keywords:
VSC-HVDC project
Offshore wind farm
Topology
Control strategy

ABSTRACT

In recent years, wind power industry has been flourishing and in China the focus has been gradually shifted from land-based to offshore wind farms. There are many advantages for offshore wind farms, such as abundant wind energy reserves, high utilization of the wind turbine capacity, not taking up land resources and so on. As wind turbine technology improves, offshore wind farms have been expanding quickly and are located further away from the onshore grid. The power transmission problem has become one of the key issues for restricting the development of offshore wind farms. For example, the technology of high voltage direct current transmission based on voltage source converter (VSC-HVDC), suitable for long-distance transmission of offshore wind energy, has become one of the current research focuses. This has resulted in higher requirements on the aspects of converter voltage level, system dynamic performance, and network power quality. The paper first discusses converter topology for offshore wind farm grid integration. Two VSC-HVDC projects for connecting offshore wind farms, which are located in Shanghai and Dalian of China, are presented in detail. Based on the two projects, the structure, control methods and application of modular multi-level converter are presented. The control strategies of VSC-HVDC are then discussed, focusing on double closed-loop vector control, direct power control, deadbeat control and the control methods for unbalanced grid voltage. This can provide good theoretical foundation for the grid integration of large offshore wind farms.

Contents

* Corresponding author. Tel.: +86 18818213963.
E-mail address: ycwjyg@163.com (J. Wu).

http://dx.doi.org/10.1016/j.rser.2014.04.061
1364-0321/

1. Introduction

Development and large-scale utilization of wind energy is of great significance and strategic value in promoting national economic development and environmental protection, solving global energy crisis and so on. This has become one of world's important strategic goals to achieve sustainable development. According to Chinese Wind Energy Association statistics, by 2013, the global total installed capacity of offshore wind power has reached about 7100 MW [1], with 428.6 MW in China. In China's "The 12th Five-Year Plan", offshore wind power is one of the development focuses. According to the preliminary provincial statistics of offshore wind power development plan, the cumulative installed capacity of offshore wind power in China is expected to reach 5 GW by 2015. The focuses of the coming development and construction will be offshore wind bases in Jiangsu and Shandong, and the promotion of offshore wind farm development in Hebei, Shanghai, Zhejiang, Fujian, Guangdong, Guangxi, Hainan provinces. The capacity is expected to reach over 30 GW in 2020 with 27.7 GW offshore and 5.1 GW inter-tidal. This article discusses the key technologies of VSC-HVDC converters for offshore wind including converter topology and control strategies of VSC-HVDC. It also provides an overview of the two offshore wind farm projects using VSC-HVDC in China, illustrating the details of the topologies, modulation methods, and voltage balancing control strategy of the modular multilevel converter (MMC) used in both projects. Finally, the VSC-HVDC control strategies for offshore wind farm system are reviewed, including double closed-loop vector control, direct power control, deadbeat control, and other non-linear control algorithms.

2. Converter topologies and its engineering applications

The two- and three-level converters are fairly maturity, having been used for offshore wind farm VSC-HVDC system [2]. However, the voltage rating of individual full-controlled switching devices, such as IGBT, is low compared to the required converter DC voltage. Thus, the bridge arm is usually composed of series-connected multiple switches, namely valve group. For three-level converters, most applications use the diode-clamped structure which was first proposed in 1981 by A. Nabae [3]. Other commonly used three-level structures include flying capacitor [4,5] and active neutral point clamped (ANPC) converters [6], etc. The VSC-HVDC projects using two- and three-level converters that have been put into operation are summarized in Table 1 [7,8].

Table 1
VSC-HVDC projects for offshore wind farm adopting two and three level converter.

Project	Topology	Capacity	DC voltage/kV
Tjaereborg	Two level	7.2 MW/−3∼+4 Mvar	±9
Direct Link		180 MW/−75∼+75 Mvar	±80
Gotland		50 MW/−30∼+30 Mvar	±80
Eagle Pass	Three level	36 MW/−36∼+36 Mvar	±15.9
Murray Link		200 MW/−150∼+140 Mvar	±150
Cross Sound		330 MW/−75∼+75 Mvar	±150
EstLink		330 MW	±150

Large-scale development and utilization of offshore wind farms increase the requirements of converters for VSC-HVDC, especially the voltage and capacity ratings. For two- and three-level converters, a large number of switches directly connected in series make the manufacturing process difficult with reduced reliability. In addition, harmonic contents of converter output voltage are high, and thus high-capacity AC filters are needed. To solve these problems, a variety of multi-level converter topologies have been proposed, including re-injected multilevel converter [9,10], ANPC multilevel [11–13], multiplex converter [14,15], and modular multilevel converter (MMC) [16–18]. Among them, the MMC composed of half-bridge structure as sub-modules is suitable for VSC-HVDC systems. This topology has been adopted by Shanghai Nanhui wind farm VSC-HVDC demonstration project and the cross-sea VSC-HVDC demonstration project being constructed in Dalian of China. The structure, operation mode and range, and operating principle are now introduced as follows.

2.1. Shanghai Nanhui VSC-HVDC demonstration project

2.1.1. Project overview

In March 2011, China's first VSC-HVDC project with completely independent intellectual property rights named China-Shanghai Nanhui VSC-HVDC demonstration project, was successfully completed and started its trial operation [17]. The converter station at Nanhui wind farm can realize dynamic voltage support, reactive power compensation, and DC power transmission. The scheme is rated at 18 MW with a DC voltage of ±30 kV and DC current of 300 A. The Length of the DC cable is 8.6 km. As shown in Fig. 1, the wind farm output is connected to the 10 kV bus at Nanhui wind farm station, and is then stepped up to 35 kV. The original double AC lines of Nanhui wind farm are connected to the 35 kV Dazhi station. After alteration, the original AC line of 35 kV bus I is disconnected. The Nanfeng converter station is then connected to this bus and its DC is connected to the Shurou converter station through DC lines. After DC/AC conversion in Shurou station, it is connected to bus I at the Dazhi station.

2.1.2. Operation mode

There are two operation states for the VSC-HVDC station, i.e., static var compensator (STATCOM) state with single-station and HVDC state with two stations. There are further five operation modes for the HVDC state by changing the operation mode of the stations and adjusting the operation state of the related substations in the grid.

Operation mode 1: Connect to grid by VSC-HVDC. Nanhui wind farm is connected to Dazhi station through Nanfeng converter station, Nanrou lines and Shurou converter station. The Zhifeng 3392 line is in reserve. It provides technical support and operational experience for future wind farm grid connection using HVDC.

Operation mode 2: AC and DC lines are of parallel operation. Nanrou line and Zhifeng 3392 line run at the same time. It

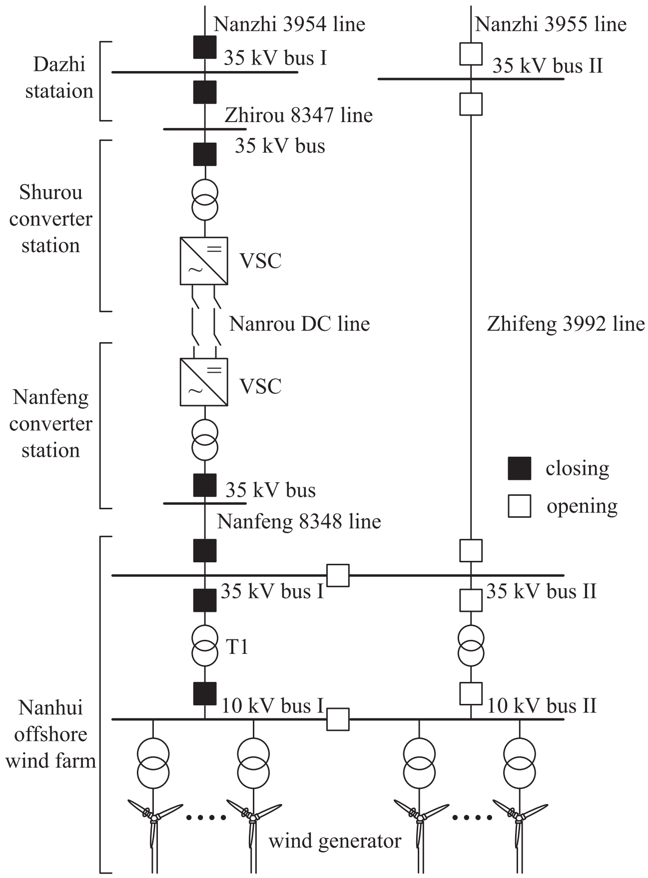


Fig. 1. Access scheme of Nanhui offshore wind farm.

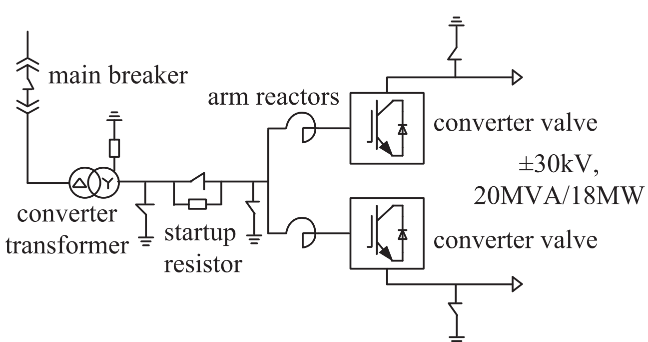


Fig. 2. The primary side structure of Nanfeng station.

provides technical support and relevant operating experience for hybrid AC-DC transmission system.

Operation mode 3: Stations at both ends run as STATCOM. The Zhifeng 3992 AC line operates and the Nanrou DC line uses as reserve. Both converter stations operate as STATCOM, involving in AC system voltage/reactive power regulation. It provides technical support and relevant operating experience for gird reactive power control.

Operation mode 4: VSC-HVDC supplies passive load. The Nanhui wind farm and Nanzhi 3955 line are disconnected and the power flow is from bus I to bus II of Dazhi station through the VSC-HVDC system, the 35 kV bus I and bus II of Nanhui wind farm, and the Zhifeng 3992 line. It provides technical support and relevant operating experience for system of supplying isolated island.

Operation mode 5: AC transmission runs independently. Nanhui wind farm is connected with the 35 kV bus II of Dazhi station through Zhifeng 3992 line. The VSC-HVDC system is out of operation. It is for VSC-HVDC system maintenance and outage.

2.1.3. Power transmission range

VSC-HVDC can independently control its active and reactive power flow. Active power adjustment range is −18 MW~+18 MW, and the reactive power range is −13 Mvar~+9 Mvar. When the output of active power is at its maximum of ±18 MW, the reactive power range is ±2 Mvar. When the output of active power is ±12 MW, the reactive power range is −13 Mvar~+9 Mvar. When the active power is within the range of 12–18 MW, the reactive power output limitation decreases according to a fixed slope.

2.1.4. Primary side structure of the converter station

The primary side structure of Nanfeng station is shown in Fig. 2. The 35 kV AC system is connected to the converter transformer through the main circuit breaker. The AC voltage is transformed to the rated converter input voltage of 31 kV which is then connected to the converter terminals through the startup resistor and arm reactors. The converter transforms AC to DC and is connected to the other converter station through the DC cables.

2.1.5. Working principle of multilevel converter

The main circuit topology of the multilevel converter is shown in Fig. 3. Each bridge arm consists of 56 sub-modules (SMs), divided into two valve towers. Each valve tower is composed of two semi-towers with cross-wiring. There are 4 layers in each semi-tower and 7 SMs in one layer. Among the 56 SMs, 48 are active running modules with the remaining eight being redundancy ones. Each SM rated voltage is 1.5 kV. L_{1-6}, between the upper and lower arms, are the arm reactors.

Each SM consists of IGBT components, sub-module controller (SMC), protecting thyristor, bypass switch, capacitors, power supply module, water-cooled pipes, etc. IGBT is the core component and there are two IGBT devices in each SM. The protecting thyristor is used for sub-modules over current protection acting as the fast bypass switch when the SM fails. This ensures that the system continues to run normally when some SMs fail. The SMC exports gate signals for the power devices. After initial charging, the voltage unbalance factor between the SMs is less than 10%. The IGBTs in each SM work complementary, and there are two states

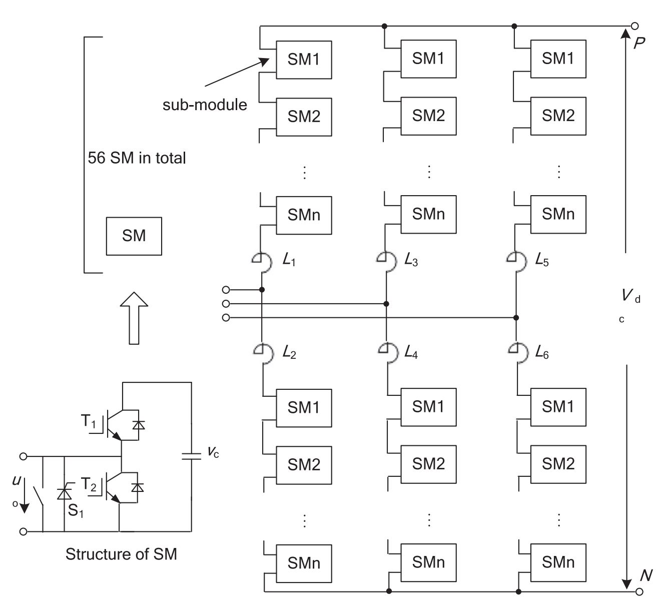


Fig. 3. Structure of three-phase VSC based on modular multilevel topology.

for each SM, on and off state. Its output voltage is two-level, v_c (on state) and 0 (off state) [18], where v_c is SM's capacitor voltage. The converter DC voltage is the sum of capacitor voltage of SMs with on state in this phase. If each SM works in pulse width modulation (PWM) mode, the AC voltage of the MMC is multi-level PWM waveform. When the number of cascade SM is large enough, the SMs can work with fundamental frequency to reduce switching losses and the AC output voltage of the MMC is multilevel staircase waveform.

2.1.6. Modulation strategy of MMC

For MMC structures with large number of SMs, the method of nearest level modulation (NLM) is usually adopted. It is a process of reference voltage qualification and approximation. The advantage of this modulation strategy is low switching frequency. Thus, the switching loss is reduced and high power devices with low switching frequency can be used, such as gate-turn-off thyristor (GTO), integrated gate commutated thyristors (IGCT) etc. The disadvantage is that harmonic contents increases with the reduction of the number of SMs. When MMC is used for high voltage VSC-HVDC system, due to the large number of SMs, the output voltage can reach tens to hundreds of levels. This would minimize the shortcomings of high harmonic contents associated with the NLM method. The NLM modulation principle is described below [19].

As shown in Fig. 4, the MMC reference signal is $m \sin(\omega t)$. For $2N+1$ level converter, the output voltage v_o^* can be approximated as:

$$v_o^* = round(2\,Nm\ \sin(\omega t)) \cdot v_{dc} \tag{1}$$

where *round* is the integral function and v_{dc} is capacitor voltage of SM (Assume that all SMs' voltage are balanced.). *round* $(2\,Nm\ \sin(\omega t))$ is the number of SMs with on state in upper arm. The upper and lower arms work complementary. When there is a SM becoming on state in lower arm, there will be one becoming off state in upper arm, and vice versa. Thus, switching state of all the SMs can be determined by the reference signal and the output stair wave is equivalent to the reference signal. In addition, the NLM strategy can keep the number of SMs at on state in each phase constant and suppress circulation current among the three phases.

2.1.7. Voltage balancing control

For MMC, the DC voltage at each phase will not be exactly equal, and therefore, there will be circulating components in the arm currents. In addition, the parameters of the DC capacitors in the SMs and their power losses vary. All the above factors can cause unbalance among the DC bus voltages of the SMs. If not tackled, this would result in different voltage stresses for the power devices, thus increasing devices' voltage rating. It could even lead to system instability. For DC capacitor voltage balancing control, there are two methods, i.e. DC capacitor voltage sorting, and adding balance component into reference signal.

(i) Method of DC capacitor voltage sorting [20]
From the NLM strategy, the number of SMs with on state is half of the total of SMs in one phase and keeps constant. This ensures the total DC voltage from the upper and lower arms in each phase to be constant. The number of SMs with on and off state in each arm is determined by the amplitude of the reference signal and the NLM strategy. The SMs' capacitor voltages are sorted according to the arm current direction and firing pulses are then allocated to each SM according to the sorting results. The allocation rule is to make the capacitors of SMs with the lowest voltage charge, and the highest voltage ones discharge.

(ii) Method of adding balance component into reference signal [21]
The circulating currents at twice the fundamental frequency can cause large fluctuation of SM capacitor voltages. Proportional regulator can be used for suppressing the circulating currents. The deviation between the DC capacitor voltages of SMs in one phase and the given value are used as the inputs of the regulator. The output of the regulator, denoted as u_{ave} is added to the reference value u'_{ref} to produce the final voltage reference signal $u_{ref} = u'_{ref} + u_{ave}$. By this way, the circulating current is suppressed and the capacitor voltage fluctuation is reduced.

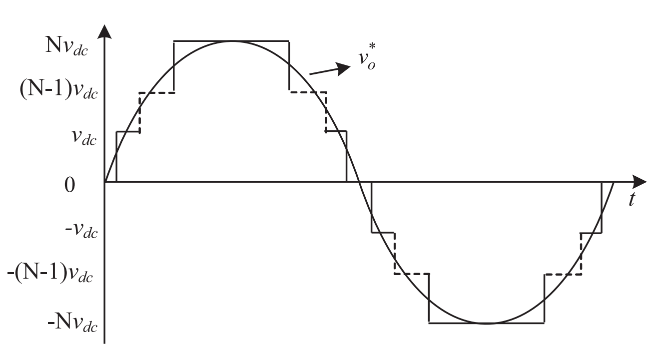


Fig. 4. The strategy of NLM.

2.2. Dalian cross-sea VSC-HVDC demonstration project [22]

2.2.1. Project overview

The project started in July 2012 and is scheduled to become operational by the end of 2016. The capacity is 1000 MVA and the DC voltage is ±320 kV. The total DC cable length is about 54 km with 35 km of submarine cable. The total investment for the project is expected to reach 5.1 billion Yuan. The sending end converter station locates at Jinjia area of Dalian, which is an extension project based on Huai river 220 kV substation. The receiving end converter station is at Donggang area of Dalian south, which is connected with Gangdong and Qingyun substation through two group lines, respectively. The VSC-HVDC system can operate with two modes, i.e. active mode, which can strengthen the transmission capacity of the Dalian urban grid, and reactive mode. If the AC transmission channel between Dalian southern grid and the main grid were to be completely disconnected (For example, tower collapses), the southern grid would run as an "isolated island" with all the power supplied from the VSC-HVDC system. It can enhance power supply reliability and transmission capacity in Dalian central area, elimination security risks of the grid.

2.2.2. Power transmission range

For the active mode, the active and reactive power can be controlled independently. Active power adjustment range is −1000 MW∼+1000 MW and reactive power is −606 Mvar∼+460 Mvar. As shown in Fig. 5, the active power output limit is ±1000 MW when the output reactive power range is 0 Mvar. When the absolute value of the active power is 700–1000 MW, the reactive power output limitation decreases according to a fixed slope.

For reactive mode, the VSC-HVDC is connected to passive network, the active and reactive power is determined by loads and the AC voltage amplitude is controlled by the converter. According to the

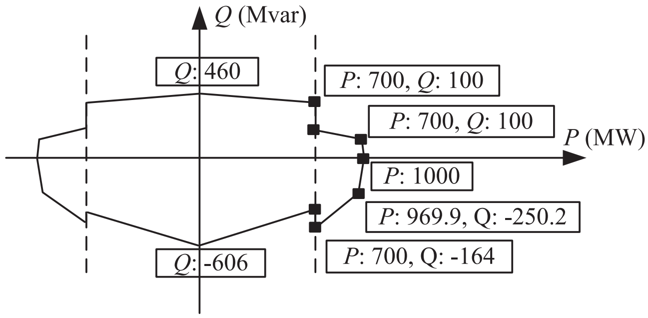


Fig. 5. Power adjustment range of VSC-HVDC station (active mode).

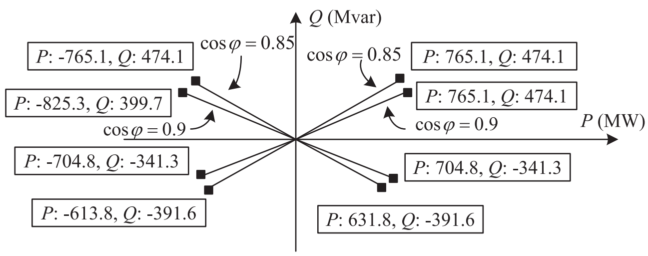


Fig. 6. Power adjustment range of VSC-HVDC station (reactive mode).

parameters of the converter's main circuit, absolute value of load power factor must be greater than 0.85, as shown in Fig. 6. When the power factor is 0.85, the maximum active power is 765 MW, whereas for a power factor of 0.9, the Maximum active power increases to 825 MW.

2.3. Nan-ao multi-terminal VSC-HVDC demonstration project [23]

The Nan-ao VSC-HVDC transmission demonstration project was put into operation in December 2013 and its investment is 1188 million yuan. As a demonstration project supported by the national 863 project, the DC side voltage is ± 160 kV and the transmission capacity is 200 MW. Both new VSC-HVDC converter stations are built near the original 110 kV Jinniu station and Qing-ao station in Nan-ao Island, respectively. The outputs of Niutou Hill, Yun-ao and Qin-ao wind farms are connected to Jinniu and Qing-ao stations for AC/DC conversion. Then, the DC power brings together at Jinniu station and is sent out through the new DC overhead cables of this island. The overhead lines are replaced by submarine cables when being away from the island and connected with Suliu station. After DC/AC conversion, it is connected with Shantou grid. The project achieves large-scale wind power on the island grid integration and is the first multi-terminal VSC-HVDC of the world.

3. Control methods of VSC-HVDC

General control algorithms of VSC-HVDC systems are usually independent to converter topology as converters only receive system control signal and act as power amplifiers to replicate the control signals on high voltage side. Therefore, the existing control strategies for two-level VSC-HVDC system can also be used for MMC based ones. For MMC, the problems of DC capacitor voltage balancing, circulating current suppressing and modulation method need further consideration. However, they have little effect on the upper VSC-HVDC system control algorithms, and belong to the lower converter control problems described in Section 2 of this paper. A lot of researches on two-level VSC-HVDC control strategies have been carried out and many useful achievements have been obtained. The common control methods for VSC-HVDC described below include: double closed-loop vector control, direct power control (DPC), nonlinear control algorithms such as dead-beat control, and intelligent control.

3.1. Double closed-loop vector control

In this method, the outer loop is power or the DC voltage loop used for controlling the transmitted active and reactive power or the DC voltage. The inner one is the current loop, used for tracking the current command signals from the outer loop regulators. This algorithm was initially developed some years ago and is relatively mature [24]. Based on the basic algorithms, further researches for unbalanced grid voltage or transient conditions have been carried out. For voltage imbalance, double vector (positive and negative sequence components) control (DVCC) is often used [25,26]. It can improve the performance of system response by controlling the negative sequence component to meet the operation requirement during unbalanced AC fault. The control structure is shown in Fig. 7. The feed-forward decoupling control method is used for inner current loop. The current command signals are determined according to the desired control objects [27].

As shown in Fig. 7, P^*, V_{dc}^* and Q^* are the given values of the active power, DC voltage and reactive power, respectively. v_{ca}, v_{cb}, v_{cc} are the desired converter output voltages. θ^+ and θ^- are the angles of positive and negative sequence voltage vectors. "u" and "i" represent the voltage and current signals, respectively. Superscript "$*$" represents the reference values. Superscript "p" and "n" represent the positive and negative sequence components, respectively. Subscript "d, q", "α,β" and "a, b, c" represent respective components of synchronous dq frame, two- and three-phase stationary frame.

Double vector control algorithm can eliminate the second harmonic of the converter DC voltage under unbalanced grid voltage conditions. However, this strategy involves the separation of positive and negative sequence components, and reference frame transformation. As the separation of the sequence components involves considerable time delay, the dynamic response can be degraded. Virtual admittance control scheme is proposed in [28] without using reference frame transformation. Generalized integrator is used and sinusoidal current can be tracked without steady-state error. References [29,30] are also based on the stationary frame using proportional-resonant (PR) controller for the inner current loop. The current command signals are calculated

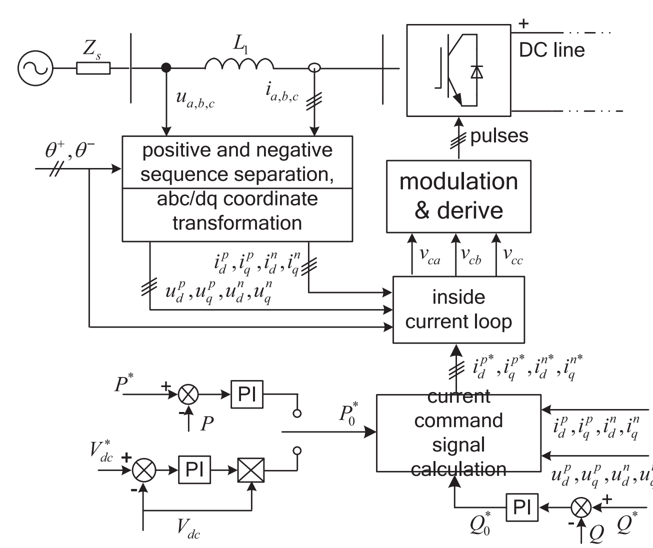


Fig. 7. Structure of double vector control under unbalanced input voltage conditions.

according to the desired control objects and it can enhance the ability of low voltage ride through (LVRT) when grid voltage drops. In [31] a near-synchronous reference frame is used to determine the positive-sequence fundamental frequency component in the input voltages. Based on this the amplitude and phase of the reference signals can be obtained. Thus, it does not need to extract either the harmonic or the negative-sequence components in the supply voltages and currents. In [32] a selective harmonic compensation method is proposed based on an improved multiple reference frame algorithm. Fast and accurate regulation of harmonic and unbalanced currents is achieved. In [33] a closed-loop observer is designed to extract the positive- and negative-sequence voltage components, based on converter mathematical model. Paper [34] uses a filter to extract the fundamental component of the grid voltage and the phase shift caused by the filter is compensated according to its characteristics. Thus, positive- and negative-sequence components can be detected with high precision. In [35] a control strategy based on model reference adaptive control and resonant filter is proposed for VSC-HVDC under unbalanced condition, without the need for sequence component detector. Paper [36] proposes an instantaneous power-regulation strategy called output-power-control method. It can obtain reference values of positive- and negative-sequence current based on the desired power. In [37], relationship between the DC link voltage ripples and the second harmonic component in the instantaneous output power is established. Based on this, a cascaded proportional-integral (PI) control scheme is developed for eliminating DC voltage fluctuation. In [38] a modified one-cycle-control (OCC) scheme is proposed to reduce the DC voltage ripple under unbalanced and distorted supply conditions without phase-locked loop (PLL) and reference frame transformation.

3.2. DPC strategy

3.2.1. Customary DPC and its improvements

DPC has the advantages of simple algorithm and fast dynamic response. By regulating the power directly, the converter current is automatically controlled. For DPC based on look-up-table and hysteresis controller, the vector selection table directly affects system performance [39]. Based on the traditional sector division and vector selection method, many improvements have been proposed. Paper [40] changes the sector division method according to the reference vector position and a new vector table is designed. In [41] the concept of output regulation subspaces is proposed and it is used to make the selection of the control inputs more accurate under balanced and unbalanced conditions. In [42] the vector table is designed according to power error and its trend.

The above methods mainly optimize the switching table of DPC and result in variable switching frequency. In [43–45], the strategy

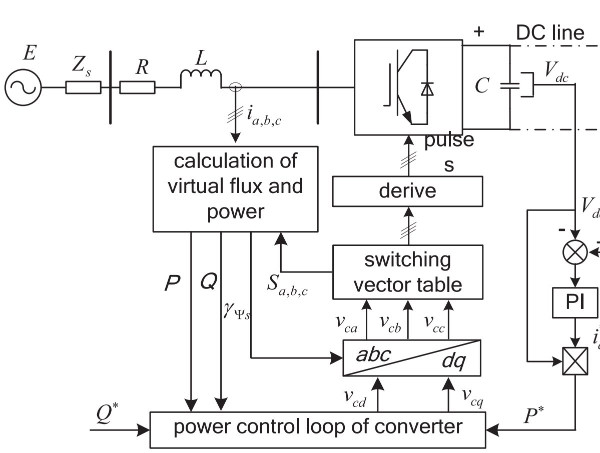


Fig. 8. Control structure of VF-DPC.

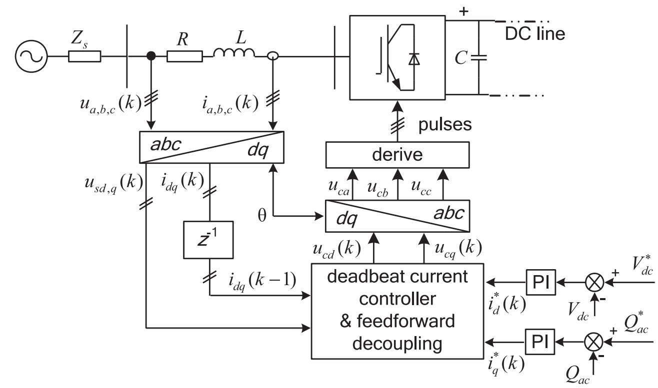


Fig. 9. Structure of dead-beat control.

of predictive DPC (P-DPC) is proposed. It selects appropriate voltage vector and calculates duty cycles directly in order to minimize the instantaneous active and reactive power errors or the sum of squared errors in every sampling period. Paper [46] utilizes the finite state model predictive control (FS-MPC) and virtual state vectors to form switching sequences within each sampling period. Such methods result in fixed switching frequency. In [47] the required converter voltage vector is calculated directly from the active and reactive power errors in a fixed half switching period to ensure constant switching frequency. Paper [48] dynamically changes the width of the hysteresis band and in paper [49] the hysteresis control is replaced by a fuzzy controller to produce near constant switching frequency.

For unbalanced grid voltage, DPC can also be applied [50]. Paper [51] derives the calculation method of converter power under unbalanced conditions. In [52] double vector control and DPC are combined to determine and track the given values of positive- and negative-sequence power. In [53] a compensation component is added to the reference signals of the conventional P-DPC to eliminate the negative sequence component from the gird current. Paper [54] proposes a new DPC method by superimposing a negative sequence component on to the power reference signals. It can keep the AC current sinusoidal with power variation. In [55], a new optimized operation strategy is proposed based on exchanged power maximization with a scalar control structure using resonant controllers. Compared with DVCC, it has better performance and increased flexibility in terms of operation modes under transient disturbances.

3.2.2. Virtual flux DPC (VF-DPC)

The concept of “virtual flux“ is resulted from “virtual motor“. The converter input voltage is considered as the induced electromotive force (EMF) generated by a motor's rotating magnetic field [56,57]. The measurement of the grid voltage and PLL can be eliminated. The position of the voltage vector is obtained through the integral relationship between voltage and flux. The integral unit is usually in the form of a low-pass filter to improve disturbance rejection. However, the initial value of the integral link is difficult to determine and system performance can degrade with inappropriate initial value. For this reason, paper [58] replaces the integral unit with a second order inertia link. In [59] an improved virtual flux observer based on an integrator with saturated amplitude limited feedback link is proposed. It eliminates the DC offset caused by wrongly selected integer initial values. Take DC voltage control for example, the control structure of VF-DPC is shown as Fig. 8, where $\gamma_{\Psi s}$ is the flux vector angle and $S_{a,b,c}$ is the switching function.

3.3. Dead-beat control

Dead-beat control is mainly used for tracking control of the converter inner current loop. It is a kind of digital control method based on discrete system model. Assuming the tracking errors can be eliminated in the next control period, the control signals are directly calculated. Thus, the controlled variable can track the given value during the next one or several periods, and the method has the advantages of high tracking speed and precision, and ease for digital implementation, etc. [60]. However, in practical applications, the A/D conversion and program execution will take some time, and control variables from previous period are still active during this period. Therefore, there is a certain delay which can bring control errors and even system instability. In order to eliminate the impact of the delay, recursive algorithm is usually used, with the converter mathematical model forward or backward one step recursion. Control variables of the next switching period can then be predicted by the current sampling values. The control structure is shown in Fig. 9, where the "k" and "$k-1$" represent sampling value of present and previous period, and z^{-1} is delay link. In principle, this method is a kind of open-loop observer. In [61] a method based on new state observer is proposed to reduce the predictive errors of open-loop state-observer used by conventional dead-beat control. In [62], a repetitive DC link voltage predictor is proposed. DC voltage is sampled multiple times within a switching period and the closed-loop observer can be constructed to eliminate the prediction errors. The same strategy is adopted by paper [63], in which the repetitive controller is used for improving current prediction accuracy. In [64] a new predictive algorithm was introduced using fuzzy control method. The prediction parameters are designed according to different reference current changes and the current overshoot is constrained and the phase delay is optimized. In [65] a deadbeat vector current controller is proposed and various methods for limiting the reference voltage vector have been investigated to maintain a proper current control.

3.4. Other control methods

There are strong nonlinear characteristics for VSC-HVDC system, and consequently, linear control methods have many limitations and non-linear control theory for VSC-HVDC has become one of the research focuses. Apart from the above DPC and dead-beat control methods, nonlinear control strategies which can be used in VSC-HVDC system include: input–output feedback linearization [66–68], passivity control [69,70], sliding mode control [71–73], back-stepping [74–76], active-disturbance rejection control (ADRC) [77–79], etc. In addition, paper [80–81] uses the inverse model controller (IMC) to trace the operating point of the DC voltage and current, whereas in [82,83] the $H\infty$ controllers are designed for constant DC voltage and power control. The dynamic performances of the nonlinear control methods are usually superior to traditional vector control. On the other hand, they increase the complexity of the controller design and the amount of required calculation is large. As many state variables may be needed the controller performance in practical applications could be affected due to parameter inaccuracy.

4. Conclusions

For converter topology used for VSC-HVDC systems, conventional two- and three-level converters and control methods are fairly mature. However, with the expansion of offshore wind farms, the converter voltage ratings increase and a large amount of switching devices connected in series would be required. This can result in a complex manufacturing process and reduced reliability. MMC using cascaded structure of half bridge has a common DC side and removes the need for connecting devices in series. Therefore, MMC is particularly suitable for large-scale offshore wind farm applications. The number of SMs cascaded in one arm is unlimited and can be configured according to the required DC voltage. The quality of output voltage is also high and passive filters can be eliminated entirely. Both offshore wind farm VSC-HVDC projects in Shanghai and Dalian of China all adopted this technology.

For the aspect of VSC-HVDC system control, the double closed-loop vector control based on PI regulators is relatively mature and easy to implement. It has been adopted by most of practical projects. However, the problems and uncertainties in optimizing regulator parameters make it difficult to obtain the optimal control effect. VF-DPC possesses advantages of fast dynamic response, reduced dependence on system parameters, and simple computation. Therefore, it is suitable for the application of VSC-HVDC system. However, the design of switching table is difficult because of too many redundant vectors when applied to multi-level converters. The improved deadbeat control eliminates the effects of sampling and calculation delay. However, the accuracy in predicting the control variables is affected by system parameters. In summary, DPC based on switching vector selection should be studied to make it more applicable for multi-level converters to achieve good system tracking and DC capacitor voltages balance. Meanwhile, if combined with dead-beat control the method can become easier for digital implementation, and can be an excellent control scheme for VSC-HVDC systems.

Acknowledgments

The authors would like to acknowledge the financing support of Key Program of The National 863 Program intelligent grid key technology R&Dprojects (2011AA05A103), the National Natural Science Foundation Item (51377105), Key Program of Shanghai High-Tech Industrialization (09-GXB113), Jiangsu Province "Six Talents Project Peak" (2010-XNY-001).

References

[1] The global offshore wind development overview of 2013, ⟨http://news.bjx.com.cn/html/20140325/499176.shtml⟩ [accessed 09.04.14].
[2] Zhixin Wang, Huaqiang Zhang. New development of wind energy generation and control strategy. Low Volt Appar 2009;19:1–7.
[3] Nabae A, Takahashi L, Akagi H. A new neutral-point clamped PWM inverter. IEEE Trans IA 1981;17(5):518–23.
[4] Lie Xu, Vassilios G. Agelidis. VSC transmission system using flying capacitor multilevel converters and hybrid PWM control. IEEE Trans Power Deliv 2007;22(1):693–702.
[5] Ke Jin, Zhijun Liu, Xiaoyang Yu, Xiaoyong Ren. A self-driven current-doubler-rectifier three-level converter with integrated magnetics. IEEE Trans Power Electron 2014;29(7):3604–15.
[6] Pulikanti SR, Dahidah MSA, Agelidis VG. Voltage balancing control of three-level active npc converter using SHE-PWM. IEEE Trans Power Deliv 2011;26 (1):258–7267.
[7] Zhi-xin Wang. Modern wind power technology and its application. Beijing: Publishing House of Electronics Industry; 2010; 1–19.
[8] Guang-fu Tang. Technology of HVDC power transmission system based on voltage source converters. Beijing: China Electric Power Press; 2010; 312–34.
[9] Liu YH, Arrillaga J, Watson NR. Capacitor voltage balancing in multi-level voltage reinjection (MLVR) converters. IEEE Trans Power Deliv 2005;20(2): 1728–37.
[10] Liu YH, Arrillaga, J, Watson, NR. Multi-level voltage reinjection—a new concept in high voltage source conversion. In: IEE proceedings on generation transmission and distribution, New Zealand: IEEE; 2004: p. 290–8.
[11] Meili J, Ponnaluri S, Serpa L, Steimer PK, Kolar JW. Optimized pulse patterns for the 5-level ANPC converter for high speed high power applications. In: Proceedings IEEE 32nd annual conference on industrial electronics, Zurich: IEEE; 2006: p. 2587–92.

[12] Barbosa P, Steimer P, Steinke J, Meysenc L, Winkelnkemper M, Celanovic N. Active neutral-point-clamped multilevel converters. In: Proceedings of IEEE 36th conference on power electronics specialists, Recife: IEEE; 2005: p. 2296–301.
[13] Chaudhuri T, Rufer A, Steimer PK. The common cross-connected stage for the 5 L ANPC medium voltage multilevel inverter. IEEE Trans. Ind. Electron. 2010;57(7):2279–86.
[14] Zhi-gang GAO, ZHANG Lei, Xun-bo FU, Jian-lin LI, Bin Zhao. A modulation method for grid-connected multiple structure inverter. Power Syst. Technol. 2008;32(20):64–7.
[15] Feng-jun Liu. Multi-level inverter technology and its application. Beijing: China Machine Press; 2007; 236–306.
[16] Rodriguez J, Bernet S, Bin Wu, Pontt JO, Kouro S. Multilevel voltage-source-converter topologies for industrial medium-voltage drives. IEEE Trans. Ind. Electron. 2007;54(6):2930–45.
[17] Weidong Qiao, Yingke Mao. Overview of shanghai flexible HVDC transmission demonstration project. East China Electric 2011;39(7):1137–40.
[18] Zhao Yan, Hu Xue-hao, Tang Guang-fu, He Zhi-yuan. A study on MMC model and its current control strategies. In: Proceedings of IEEE 2nd international symposium on power electronics for distributed generation systems, Beijing: IEEE; 2010: p. 259–64.
[19] Perez M, Rodriguez J, Pontt J, Kouro S. Power distribution in hybrid multi-cell converter with nearest level modulation. In: Proceedings of IEEE international symposium on industrial electronics, Valparaiso: IEEE; 2007: p. 736–41.
[20] Zhongqi Liu, Song Qiang, Wenhua Liu. VSC-HVDC system based on modular multilevel converters. Autom Electric Power Syst. 2010;34(2):53–8.
[21] Hagiwara M, Akagi H. Control and experiment of pulsewidth-modulated modular multilevel converters. IEEE Trans Power Electron 2009;24(7): 1737–46.
[22] Wei-chun Ge, Hong-qun Gu, Zhi-yuan He. Overview on dalian flexible HVDC transmission demonstration project. Northeast Electric Power Technol 2012;33(2):1–4.
[23] VSC-HVDC engineering for large-scale wind farms locate at Nan-ao Island. 〈http://www.sasac.gov.cn/n1180/n1226/n2410/n314274/15646769.html〉; [accessed 09.04.14].
[24] Wang W, Barnes M. Power flow algorithms for multi-terminal VSC-HVDC with droop control. IEEE Trans Power Syst 2014;99:1–10.
[25] Moawwad A, El Moursi MS, Xiao W, Kirtley JL. Novel configuration and transient management control strategy for VSC-HVDC. IEEE Trans. Power Syst. 2014;99:1–11.
[26] Lie Xu, Andersen BR, Cartwright P. VSC transmission operating under unbalanced AC conditions-analysis and control. IEEE Trans Power Deliv 2005;20(1):427–34.
[27] Yongsug Suh, Yuran Go, Dohwan Rho. A comparative study on control algorithm for active front-end rectifier of large motor drives under unbalanced input. IEEE Trans Ind Appl 2011;47(3):1419–31.
[28] Xiao-jie Wu, Ying-jie Wang, Rong-wu Zhu, Peng Dai. Virtual admittance control scheme of three-phase PWM rectifier under unbalanced input voltage condition. Electric Power Autom Equip 2010;30(3):35–9.
[29] Zou Zhixiang, Wang Zheng, Cheng Ming. Modeling, analysis, and design of multifunction grid-interfaced inverters with output LCL filter. IEEE Trans Power Electron 2014;29(7):3830–9.
[30] Li Zixin, Yaohua, Wang Ping, Zhu Haibin, Liu Congwei, Xu Wei. Control of three-phase boost-type PWM rectifier in stationary frame under unbalanced input voltage. IEEE Trans Power Electron 2010;25(10):2521–30.
[31] Peng Xiao, Corzine KA, Venayagamoorthy GK. Cancellation predictive control for three-phase PWM rectifiers under harmonic and unbalanced input conditions. In: Proceedings of 32nd Annual Conference on Industrial Electronics, Rolla MO: IEEE; 2006: p. 1816–21.
[32] Peng Xiao, Corzine KA, Venayagamoorthy GK. Multiple reference frame-based control of three-phase PWM boost rectifiers under unbalanced and distorted input conditions. IEEE Trans Power Electron 2008;23(4):2006–17.
[33] Lee K, Jahns TM, Lipo TA, Blasko V, Lorenz RD. Observer-based control methods for combined source-voltage harmonics and unbalance disturbances in PWM voltage-source converters. IEEE Trans Ind Appl 2009;45(6):2010–21.
[34] Gui-bin Zhang, Zheng Xu, Guang-zhu Wang. Study and simulation of real-time detecting method for fundamental positive sequence, Proceedings of the Csee negative sequence components and harmonic components based on space vector; 2001, 21(10):p. 1–5.
[35] Leon AE, Mauricio JM, Solsona JA, Gomez-Exposito A. Adaptive control strategy for VSC-based systems under unbalanced network conditions. IEEE Trans Smart Grid 2010;1(3):311–9.
[36] Bo Yin, Oruganti R, Panda SK, Bhat AKS. An output-power-control strategy for a three-phase PWM rectifier under unbalanced supply conditions. IEEE Trans Ind Electron 2008;55(5):2140–51.
[37] Wu XH, Panda SK, Xu JX. Analysis of the Instantaneous power flow for three-phase PWM boost rectifier under unbalanced supply voltage conditions. IEEE Trans Power Electron 2008;23(4):1679–91.
[38] Yi Tang, Poh Chiang Loh, Peng Wang, Fook Hoong Choo. One-cycle controlled three-phase PWM rectifiers with improved regulation under unbalanced and distorted input voltage conditions. IEEE Trans Power Electron 2010;25 (11):2786–96.
[39] Holtz J. Pulsewidth modulation for electronic power conversion. In: Proceedings of the IEEE, Wuppertal University; 1994: 82(8):p. 1194–214.
[40] Wei Chen, Xu-dong Zou, Jian Tang, Zhao-xia Huang, Fen Li, Zhen-xing Wu, et al. DPC modulation mechanism of three-phase voltage source PWM rectifiers. Proc CSEE 2010;30(3):35–41.
[41] Escobar G, Stankovic AM, Carrasco JM, Galvan E, Ortega R. Analysis and design of direct power control (DPC) for a three phase synchronous rectifier via output regulation subspaces. IEEE Trans Power Electron 2008;18(3):823–30.
[42] Sato A, Noguchi T. Voltage-source PWM rectifier–inverter based on direct power control and its operation characteristics. IEEE Trans Power Electron 2011;26(5):1559–67.
[43] Yang Xingwu, Jiang Jianguo. Predictive direct power control for three-phase voltage source PWM rectifiers. Proc CSEE 2011;31(3):34–9.
[44] Antoniewicz P, Kazmierkowski MP. Virtual-flux-based predictive direct power control of ACDC converters with online inductance estimation. IEEE Trans Ind Electron 2008;55(12):4381–90.
[45] Jiabing Hu. Improved dead-beat predictive DPC strategy of grid-connected DC–AC converters with switching loss minimization and delay compensations. IEEE Trans Ind Inf 2013;9(2):728–38.
[46] Vazquez S, Leon JI, Franquelo LG, Carrasco JM, Martinez O, Rodriguez J, et al. Model predictive control with constant switching frequency using a discrete space vector modulation with virtual state vectors. In: IEEE international conference on industrial technology, Seville; 2009: p. 1–6.
[47] Dawei Zhi, Lie Xu, Williams BW. Improved direct power control of grid-connected DC/AC converters. IEEE Trans Power Electron 2009;24(5):1280–92.
[48] Serpa LA, Round SD, Kolar JW. A Virtual-Flux Decoupling Hysteresis Current Controller for Mains Connected Inverter. Power Electronics Specialists Conference, Zurich: IEEE; 2006: p. 1–7.
[49] Bouafia A, Krim F, Gaubert JP. Fuzzy-logic-based switching state selection for direct power control of three-phase PWM rectifier. IEEE Trans Ind Electron 2009;56(6):1984–92.
[50] Kazmierkowski MP, Jasinski M, Wrona G. DSP-based control of grid-connected power converters operating under grid distortions. IEEE Trans Ind Inf 2011;7 (2):204–11.
[51] Suh Yongsug, Lipo TA. Modeling and analysis of instantaneous active and reactive power for PWM AC/DC converter under generalized unbalanced network. IEEE Trans Power Deliv 2006;21(3):1530–40.
[52] Roiu D, Bojoi R, Limongi LR, Tenconi A. New stationary frame control scheme for three-phase PWM rectifers under unbalanced voltage dips conditions. In: Proceedings of IEEE industry applications society annual meeting, Torino; 2008: p. 1–7.
[53] Lei Shang, Dan Sun, Jiabing Hu,Yikang He. Predictive direct power control of grid-connected voltage-sourced converters under unbalanced grid voltage conditions. In: Proceedings of IEEE international conference on electrical machines and systems, Hangzhou; 2009: p. 1–5.
[54] Eloy-Garcia J, Arnaltes S, Rodriguez-Amenedo JL. Direct power control of voltage source inverters with unbalanced grid voltages. IET Power Electron 2008;1(3):395–407.
[55] Etxeberria-Otadui I, Viscarret U, Caballero M, Rufer A, Bacha S. New optimized PWM VSC control structures and strategies under unbalanced voltage transients. IEEE Trans Ind Electron 2007;54(5):2902–14.
[56] Qiang Geng, Chang-liang Xia, Yan Yan, Wei Chen. Direct power control in constant switching frequency for PWM rectifier under unbalanced grid voltage conditions. Proc CSEE 2010;30(36):79–85.
[57] Gonzalez Norniella J, Cano JM, Orcajo GA, Rojas CH, Pedrayes JF, Cabanas MF, et al. Improving the dynamics of virtual-flux-based control of three-phase active rectifiers. IEEE Trans Ind Appl 2014;61(1):177–87.
[58] Wei Chen. Research and realization on direct power control of three-phase voltage-source PWM rectifier [Ph.D. dissertation]. Hu Bei, China: Dept. Elect. Eng. Huazhong Univ. of Science and Technology; 2009.
[59] Feng-jiang Wu, Wang Zhi-wen, Li Sun. Improved virtual flux oriented vector control of PWM rectifier. Electric Mach Control 2008;12(5):504–8.
[60] Yong Yang, Yi Ruan, Guo-xiang Wu, Jing-bo Zhao. Deadbeat decoupling control of three-phase grid-connected inverters based on DPWM1. Trans China Electrotech Soc 2010;25(10):101–7.
[61] Chun-long Li, Song-hua Shen, Jia-lin Lu, Jian-rong Zhang, Xiao-qing Bai, Tao Shi. Deadbeat control for current loop of PWM rectifier based on state-observer. Trans China Electrotech Soc 2006;21(12):84–9.
[62] Hui Ouyang, Kai Zhang, Peng-ju Zhang, Yong Kang, Jian Xiong. Repetitive compensation of fluctuating DC link voltage for railway traction drives. IEEE Trans Power Electron 2011;26(8):2160–71.
[63] Ji-lei Gao, Xian-jin Huang, Fei Lin, Qionglin Zheng. Deadbeat control strategy for PWM rectifiers based on repetitive observer. Trans China Electrotech Soc 2010;25(6):47–54.
[64] Bo Qu, Xiao-yuan Hong, Zheng-yu Lv. Application of fuzzy control theory to deadbeat control scheme in three-phase pulse width modulation rectifier. Proc CSEE 2009;29(15):50–4.
[65] Ottersten R, Svensson J. Vector current controlled voltage source converter-deadbeat control and saturation strategies. IEEE Trans Power Electron 2002;17 (2):279–85.
[66] Mohamed A. Eltawil, Zhengming Zhao. Grid-connected photovoltaic power systems: Technical and potential problems—a review. Renew Sustain Energy Rev 2010;14(1):112–29.
[67] Yong Li, Fang Liu, Christian Rehtanz, Luo Long-fu, Cao Yi-jia. Dynamic output-feedback wide area damping control of HVDC transmission considering signal time-varying delay for stability enhancement of interconnected power systems. Renew Sustain Energy Rev 2012;16(8):5747–59.
[68] Bidram A, Davoudi A, Lewis FL, Guerrero JM. Distributed cooperative secondary control of microgrids using feedback linearization. IEEE Trans Power Syst 2013;28(3):3462–70.

[69] Nema Pragya, Nema RK, Rangnekar Saroj. A current and future state of art development of hybrid energy system using wind and PV-solar: a review. Renew Sustain Energy Rev 2009;13(8):2096–103.
[70] Tzann-Shin Lee. Lagrangian modeling and passivity-based control of three-phase AC/DC voltage-source converter. IEEE Trans Ind Electron 2004;51 (4):892–902.
[71] Mohammad Monfared, Saeed Golestan. Control strategies for single-phase grid integration of small-scale renewable energy sources: a review. Renew Sustain Energy Rev 2012;16(7):4982–93.
[72] Domínguez-García José Luis, Gomis-Bellmunt Oriol Gomis, Bianchi Fernando D, Sumper Andreas. Power oscillation damping supported by wind power: a review. Renew Sustain Energy Rev 2012;16(7):4994–5006.
[73] Jia-bing Hu, Lei Shang, Yi-kang He, ZQ Zhu. Direct active and reactive power regulation of grid-connected DC AC converters using sliding mode control approach. IEEE Trans Power Electron 2011;26(1):210–22.
[74] Kamil Kaygusuz. Energy for sustainable development: A case of developing countries. Renew Sustain Energy Rev 2012;16(2):1116–26.
[75] Mousazadeh H, Keyhani A, Javadi A, Mobli H, Abrinia K, Sharifi A. A review of principle and sun-tracking methods for maximizing solar systems output. Renew Sustain Energy Rev 2009;13(8):1800–18.
[76] Bao-Li Ma, Wen-Jing Xie. Comments on "Comments on Asymptotic Back-stepping Stabilization of an Underactuated Surface Vessel". IEEE Trans Control Syst Technol 2014;22(2):822–4.
[77] Yuan-bo Guo, Xin Zhou, Xiao-hua Zhang, Hong-jun Chen. Auto-disturbance rejection control for three-phase voltage-type PWM rectifier. Autom Electric Power Syst 2011;35(16):87–93.
[78] Ortega R, Figueres E, Garcerá G, Trujillo CL, Velasco D. Control techniques for reduction of the total harmonic distortion in voltage applied to a single-phase inverter with nonlinear loads: Review. Renew Sustain Energy Rev 2012;16 (3):1754–61.
[79] Zhixin Wang, Chuanwen Jiang, Qian Ai, Chengmin Wang. The key technology of offshore wind farm and its new development in China. Renew Sustain Energy Rev 2009;13(1):216–22.
[80] Guibin Zhang, Zheng Xu, Guang zhu Wang. Steady-state model and its nonlinear control of VSC-HVDC system. Proc CSEE 2002;22(1):17–22.
[81] Carmen Lucia Tancredo Borges. An overview of reliability models and methods for distribution systems with renewable energy distributed generation. Renew Sustain Energy Rev 2012;16(6):4008–15.
[82] Hai-feng Liang, Song Wang, Geng-yin Li, Cheng-yong Zhao. Design of H_∞ controller for VSC-HVDC systems. Power Syst Technol 2009;33(9):35–9.
[83] Baños R, Manzano-Agugliaro F, Montoya FG, Gil C, Alcayde A, Gómez J. Optimization methods applied to renewable and sustainable energy: a review. Renew Sustain Energy Rev 2011;15(4):1753–66.